Ultrasound in Med. & Biol., Vol. 30, No. 10, pp. 1365–1371, 2004

0301-5629/04/$–see front matter

ELSEVIER

doi:10.1016/j.ultrasmedbio.2004.08.012

● *Original Contribution*

FEASIBILITY STUDY: REAL-TIME 3-D ULTRASOUND IMAGING OF THE BRAIN

STEPHEN W. SMITH,* KENGYEH CHU,* SALIM F. IDRISS,† NIKOLAS M. IVANCEVICH,* EDWARD D. LIGHT* and PATRICK D. WOLF*

*Department of Biomedical Engineering, Duke University, Durham, NC, USA; and †Department of Pediatrics, Duke University Medical Center, Durham, NC, USA

(*Received* 19 *February* 2004, *revised* 11 *August* 2004, *accepted* 17 *August* 2004)

Abstract—We tested the feasibility of real-time, 3-D ultrasound (US) imaging in the brain. The 3-D scanner uses a matrix phased-array transducer of 512 transmit channels and 256 receive channels operating at 2.5 MHz with a 15-mm diameter footprint. The real-time system scans a 65° pyramid, producing up to 30 volumetric scans per second, and features up to five image planes as well as 3-D rendering, 3-D pulsed-wave and color Doppler. In a human subject, the real-time 3-D scans produced simultaneous transcranial horizontal (axial), coronal and saggital image planes and real-time volume-rendered images of the gross anatomy of the brain. In a transcranial sheep model, we obtained real-time 3-D color flow Doppler scans and perfusion images using bolus injection of contrast agents into the internal carotid artery. (E-mail: stephen.w.smith@duke.edu) © 2004 World Federation for Ultrasound in Medicine & Biology.

Key Words: **Two-dimensional array, Volumetric ultrasound imaging, Transcranial sonography.**

INTRODUCTION

Over the last decade, with the availability of color flow Doppler combined with effective contrast agents, a renaissance has occurred in the evaluation of cerebrovascular disease using transcranial sonography, despite of the image-degrading properties of the skull. Extensive recent reviews have described the role of ultrasound (US) in the evaluation of stroke and other pathologies of the intracranial vascular system (Bogdahn et al.1998; Gahn and von Kummer 2001) as well as the brain parenchyma (Berg and Becker 2002). A standardized examination procedure includes the use of a phased-array sector scanner, operating at approximately 2 MHz, applied to the temporal acoustic windows of the skull, combined with contrast agents and color flow Doppler. There is evidence of the value of transcranial sonography for emergency room screening and as a low-cost, bedside method for evaluation and management of patients with neurologic disease (Gahn and von Kummer 2001). Furthermore, there is continuing progress in the measurement of cerebral perfusion with new US contrast agents and harmonic imaging techniques (Eyding et al. 2003).

Recently, there have also been descriptions of 3-D transcranial sonographic imaging using mechanical rotation of the phased-array transducer combined with cardiac gating and subsequent off-line image segmentation and reconstruction (Bauer et al. 1998; Schlachetzki et al. 2001). The overall process requires several minutes. Bauer et al. (1998) listed advantages of 3-D transcranial sonography, including enhanced visualization, less operator-dependence, improved retrospective analysis and volumetric measurements.

During the last decade, we have concentrated our efforts on real-time 3-D US imaging, primarily for cardiac applications. Originally developed at Duke University (Smith et al. 1991; von Ramm et al. 1991), the current commercial 3-D system uses a 2-D matrix phased-array transducer of $N \times N$ elements to steer and focus the US beam over a 65° pyramid to produce real-time volumetric scans at rates up to 30 volumes/s (Volumetrics Medical Imaging, VMI, Durham, NC). Real-time display options include up to five image planes oriented at any desired angle and depth within the pyramidal scan, as well as real-time 3-D rendering, real-time 3-D pulsed-wave and 3-D color flow Doppler. Clinical and animal evaluations

Address correspondence to: Stephen W. Smith, Professor, Department of Biomedical Engineering, Box 90281, Duke University, Durham, NC 27708 USA. E-mail: stephen.w.smith@duke.edu

have shown potential advantages over conventional 2-D scanners for measurement of cardiac ventricular volumes (Schmidt et al. 1999; Qin et al. 2000), reduced scanning times in dobutamine stress echo examinations (Ahmad et al. 2001), measurement of peak left ventricular flow velocities (Tsujino et al. 2001) and guidance of right ventricular endomyocardial biopsy (Firek et al. 2000).

We have also had a long-time interest in transcranial sonography. To our knowledge, in 1978, we described the first real-time B-scan of the brain (Smith et al. 1978b). We also investigated adaptive signal processing techniques to correct the image-degrading effects of the skull bone (Smith et al. 1978a, 1986).

In this paper, we describe a feasibility study of real-time 3-D imaging of the brain. In a human subject, the real-time 3-D scans produce simultaneous transcranial horizontal (axial), coronal and saggital image planes of the brain, as well as any desired oblique views and real-time volume-rendered images within the 3-D pyramid. In a transcranial sheep model, we obtained real-time 3-D color flow Doppler scans and perfusion images using a bolus injection of contrast agents into the internal carotid artery.

METHODS

Volumetric scanner system

The commercial VMI US scanner generates a real-time 3-D pyramidal scan of 65°, using as many as 512 transmitters and 256 receive channels. The scanner uses 16:1 receive-mode parallel processing to generate 4096 B-mode image lines at up to 30 volumes per s. Figure 1 shows a schematic of the matrix phased-array transducer producing the pyramidal scan with two simultaneous orthogonal B-mode image planes (perpendicular to the transducer array) and two C-mode planes (parallel to the array). Alternatively, each image plane can be inclined at any desired angle. By integrating and spatially filtering between two user-selected planes (e.g., the C-mode planes), the system also displays real-time 3-D rendered images. In the following figures, arrows to the side of the B-scans define the C-mode planes. In the figures where rendered images are shown, the rendered volume is defined by the data between arrowheads to the side of (or below) the B-scans. Blunt arrows show the relative orientations of the B-scan planes.

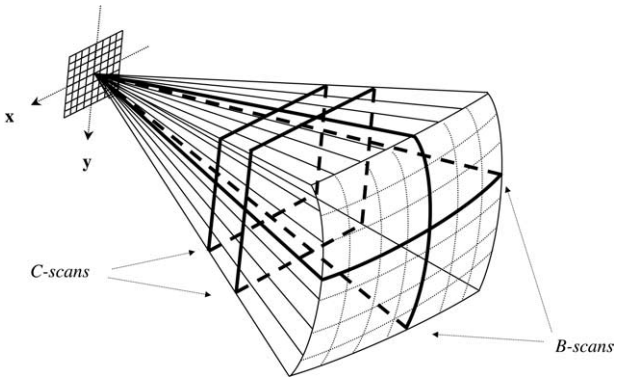

Fig. 1. Schematic of the pyramidal scan from matrix array. Bold lines indicate possible display planes. By integrating and spatially filtering between two user-selected planes, real-time 3-D rendered images are displayed.

The transcranial transducer used in this feasibility study consisted of a $40 \times 40 = 1600$ element sparse 2-D array operating at 2.5 MHz, previously described by Light et al. (1998). The active elements of the array, shown in Fig. 2a, include 440 transmit elements and 256 receive elements with a minimum interelement spacing of 0.35 mm and total aperture diameter = 13 mm. Figure 2b is a photograph of the matrix array probe, closely resembling a conventional 2-D phased-array cardiac probe.

Figure 3 illustrates the real-time 3-D rendering display option of the scanner. We scanned an US contrast detail phantom (Smith et al. 1985, ATS Laboratories, Norwalk, CT; model 532B) that includes stepped cones (i.e., stacked cylindrical targets) 5, 10 and 20 mm in diameter, of various contrasts. Figure 3 shows simultaneous image planes from an 8-cm deep 3-D scan of a hyperechogenic cone (contrast = +12 dB), including long axis (Fig. 3a) and short axis (Fig. 3b) sector B-scans of the 20-mm cylinder. In addition, Fig. 3c shows a simultaneous 3-D rendered image selected from the pyramidal volume as shown by the arrowheads in Fig. 3a and b. The real-time rendered image can be viewed from any angle by rotating the image about the x, y and z axes.

Figure 4 illustrates the C-scan display option from a 14-cm deep 3-D scan of a hypoechogenic cone (contrast = −12 dB), showing a B-scan of the cone long axis (Fig. 4a) and two simultaneous C-scans (Fig. 4b and c) of the cone short axis taken at the 5-mm and 10-mm diameter cylinders. Figure 4 also illustrates the image quality of the scanner, in which the 5-mm diameter lumen of the cylinder is easily detectable in the C-scan, where the spatial resolution in both *x* and *y* directions (shown in Fig. 1) is determined by the lateral beam width of the matrix array transducer, with no contribution from the axial resolution.

Human study

One author, a 56-year-old 100-kg man, scanned his head from the conventional temporal window (Becker and Griewing 1998), aligning the probe so that the x and y axes of the matrix array in Fig. 1 roughly corresponded to the axial and coronal planes through the skull. In this way, the C-scan planes parallel to the face of the transducer corresponded to the saggital planes. Selected im-

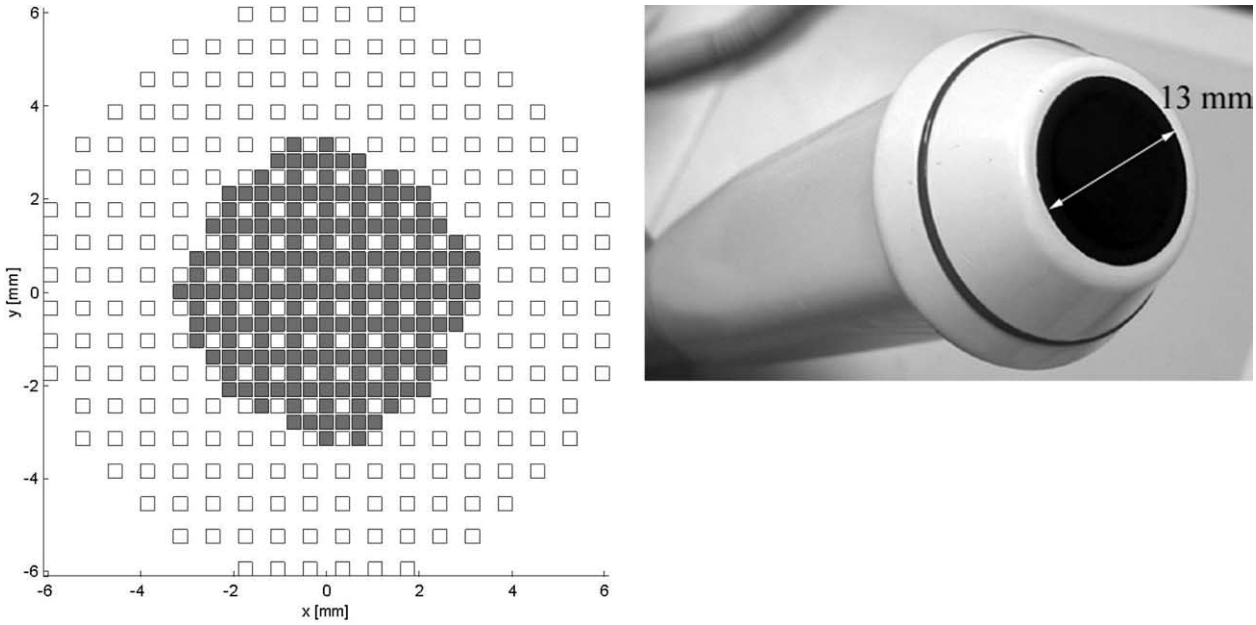

Fig. 2. (a) Schematic of matrix array geometry. (b) Photograph of 2.5-MHz matrix array transducer probe. (□) shared element; (■) transmit-only element.

age planes from the 3-D scans were matched with the best estimates of the corresponding anatomical slices from a cross-sectional brain atlas (Roberts and Hanaway. 1970).

Animal model

One sheep was used in this study. The animal experiment complied with legal requirements and institutional guidelines. Anesthesia was induced with ketamine hydrochloride, 15 to 22 mg/kg IM, and maintained with isoflurane gas, 1 to 5%, delivered through a nose cone. After peripheral IV access was obtained, the animal was placed on its back on a heated thermal pad. A tracheostomy was performed and the animal was mechanically ventilated with 95 to 99% oxygen. To prevent rumenal typany, a nasogastric tube was passed into the stomach. A femoral arterial line was placed on the left side via a percutaneous puncture. Electrolyte and respirator adjustments were made, based on serial electrolyte and arterial blood gas measurements. An IV maintenance fluid with 0.9% sodium chloride was infused continuously. Blood pressure, lead II electrocardiogram and temperature were continuously monitored throughout the procedure.

The left side of the head was shaved. Under fluoroscopic guidance with bolus injections of radiographic contrast agent (Renographin® 60, Bracco Diagnostics, Princeton, NJ), a 6-Fr catheter was placed in the right femoral artery via percutaneous puncture and advanced retrograde through the aorta and then prograde into the right internal carotid artery (ICA). Ultrasound scanning with 3-D color Doppler was performed through the left

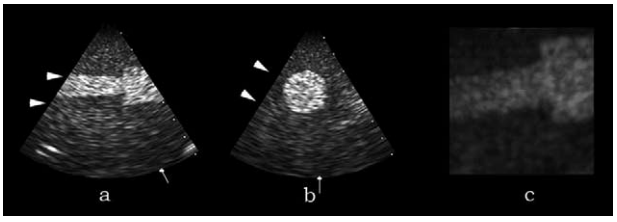

Fig. 3. Simultaneous image planes of a hyperechogenic cone (contrast = +12 dB) including (a) long-axis and (b) short-axis sector B-scans of the 20-mm cylinder. Orientations of planes are shown by blunt arrows. (c) Simultaneous 3-D rendered image segmented from the pyramidal volume as shown by the arrowheads in (a) and (b).

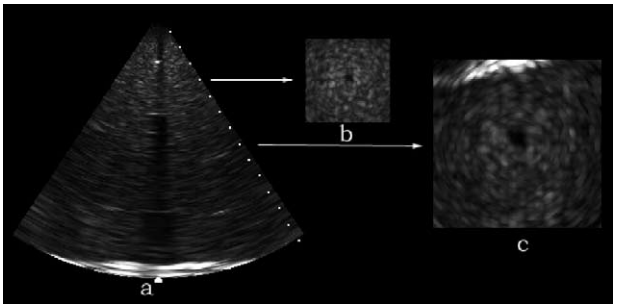

Fig. 4. 3-D scan of a hypoechogenic cone (contrast = −12 dB) showing (a) B-scan of the cone long axis, and (b) and (c) two simultaneous C-scans of the cone short axis taken at the 5-mm and 10-mm diameter cylinders. Arrows = depth of C-scans.

temple. During 3-D color flow Doppler imaging, a rapid bolus injection (1 s) of US contrast agent (10 mL of 400 mg/mL, Levovist®, Shering AG) was made through the catheter into the right ICA. In a second experiment, 100 mL of normal saline solution was agitated for 1 min and then injected through the catheter into the right ICA during 3-D color Doppler imaging.

The sheep was euthanized by a bolus injection of KCl to arrest the heart while under anesthesia. Immediately after euthanization, a 7 cm × 4 cm segment of the top of the skull was removed with a surgical saw, creating an opening to the top anterior of the brain to enable "best case" 3-D US scans of the sheep brain. Figure 5 shows the results of a 3-D scan with a 6-cm scan depth. Three simultaneous views of the sheep brain are shown including: 1. a coronal sector B-scan (Fig. 5a) compared with a coronal section from an atlas of the sheep brain (Fig. 5b) (Johnson et al. 2003; The navigable atlas of the sheep brain. NSF grants IBN 0131267, 0131826, 0131028.); 2. a saggital sector B-scan (Fig. 5c); and 3. a real-time 3-D rendering of the ventricles from a coronal view (Fig. 5d). In the coronal section (Fig. 5a), the base of the skull at a depth of 3.5 cm, the anterior portions of the lateral ventricles and the upper and lower midcerebral fissures are identified compared with the anatomical section (Fig. 5b).

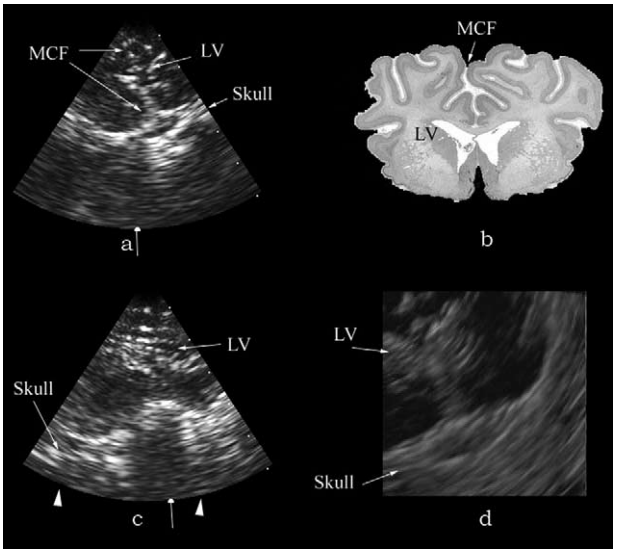

Fig. 5. Three simultaneous views from 3-D scan of post mortem sheep brain through an opening in the skull are shown including: (a) Coronal sector B-scan compared with (b) coronal section from an atlas of the sheep brain (Johnson et al. 2003, reprinted with permission), (c) saggital sector B-scan and (d) real-time 3-D rendering of the ventricles from a coronal view. In the coronal section (a), the base of the skull at a depth of 3.5 cm, the anterior portions of the lateral ventricles (LV) and the upper and lower midcerebral fissures (MCF) are identified, compared with the anatomical section (b). The saggital sector B-scan (c) shows echoes from the cortex and corpus callosum, as well as the lumen of the hypoechogenic lateral ventricle (LV). Blunt arrows = orientation of B-scans; arrowheads = volume of rendered image.

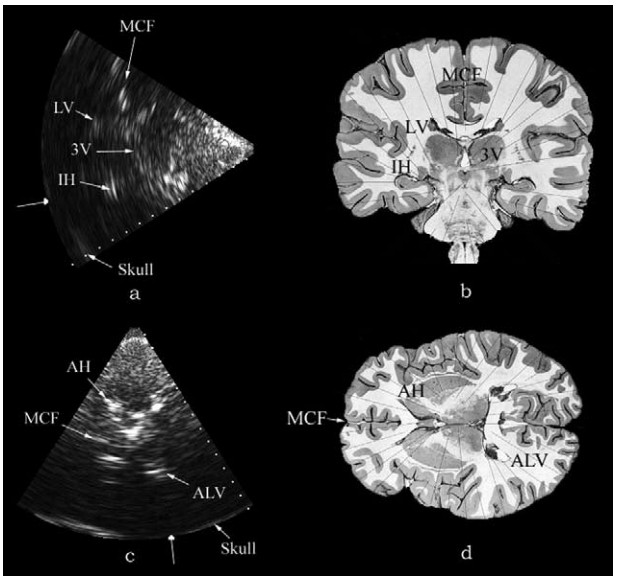

Fig. 6. Two simultaneous transcranial views, coronal and horizontal from a 14-cm deep 3-D scan. (a) Coronal view through the body of the lateral ventricles, including midcerebral fissure (MCF), lateral ventricles (LV), third ventricle (3V) and inferior horns of the lateral ventricles (IH) compared with (b) coronal anatomical slice through the posterior commissure (Roberts and Hanaway 1970, reprinted with permission). (c) Horizontal image plane from the 3-D scan compared with (d) anatomical section through the midlevel of the diencephalon. (c) The contralateral skull bone, echoes from the midcerebral fissure (MCF), anterior horns of the lateral ventricles (AH) and atria of the lateral ventricles (ALV). Blunt arrows = orientation of B-scans.

The 3-D rendered image (Fig. 5d) contains more information than the B-scan (Fig. 5a), yielding additional structures near the ventricles as well as showing the curvature of the skull bone. The saggital sector B-scan (Fig. 5c) was taken near the midline of the brain and shows echoes from the cortex and corpus callosum, as well as the lumen of the hypoechogenic lateral ventricle.

RESULTS

Human study

Figure 6 shows two simultaneous transcranial views, coronal and horizontal from a 14-cm deep 3-D scan directed toward the body of the lateral ventricles, along with the corresponding anatomical slices from the brain atlas (Roberts and Hanaway 1970). Figure 6a shows a coronal view through the body of the lateral ventricles compared with a coronal anatomical slice through the posterior commissure (Fig. 6b). Note that the sector scan image (Fig. 6a) has been rotated 90°, to place

the top of the brain at the top of the figure. In Fig. 6a, one can see the midcerebral fissure, lateral ventricles, third ventricle and inferior horns of the lateral ventricles, in comparison with the anatomical section.

Figure 6c shows a horizontal image plane from the 3-D scan, compared with an anatomical section through the midlevel of the diencephalon (Fig. 6d). Figure 6c shows the contralateral skull bone, echoes from the midcerebral fissure, anterior horns of the lateral ventricles and atria of the lateral ventricles.

Figure 7 shows four simultaneous transcranial views, coronal, horizontal, 3-D rendering and saggital, from a 14-cm deep 3-D scan directed toward the posterior portions of the lateral ventricles, along with the corresponding anatomical slices from the brain atlas. Figure 7a shows a coronal view through the atria of the lateral ventricles compared with a coronal anatomical slice through the fourth ventricle (Fig. 7b). In Fig. 7a, one can see the midcerebral fissure and the atria of the lateral ventricles in comparison with the anatomical section (Fig. 7b).

Figure 7c shows a horizontal image plane from the 3-D scan compared with an anatomical section through the putamen (Fig. 7d). Figure 7c shows the contralateral skull bone, echoes from the body, and atria of the lateral ventricles. Note that the hypoechogenic lumen of the ventricles can be seen in both Fig. 7a and c.

Figure 7e shows a real-time 3-D rendered image of the body of the lateral ventricles corresponding to peering through a thick horizontal slice through the ventricles. In the brain atlas sections, this is equivalent to looking from Fig. 7f, a section from the inferior limit of the corpus callosum, to Fig. 7d. There is clear evidence of additional information in the rendered view (Fig. 7e) compared with the B-scan horizontal image (Fig. 7c).

Figure 7g shows a slightly tilted C-scan roughly parallel to the transducer face, which corresponds to a saggital view through the brain, compared with a saggital section near the midline of the brain (Fig. 7h). The image shows the hypoechogenic lumen of the body of the lateral ventricle, as well as echoes from the wall of the ventricle and corpus callosum. Note that the spatial resolution in the transskull C-scan (saggital view) is significantly worse than that of the C-scan of Fig. 4b and the B-scans of Fig. 7a and c. The resolution in the C-scan, determined by the transducer lateral resolution in both x and y directions, has been significantly degraded by the skull bone, whereas, in the B-scans (Fig. 7a and c), the axial resolution of the depth direction is not adversely affected by the skull.

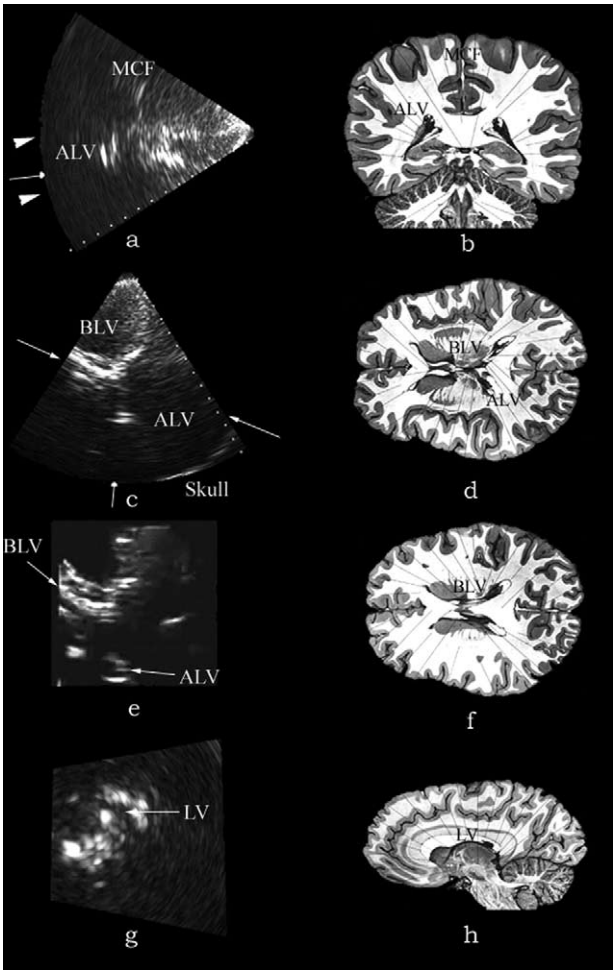

Fig. 7. Four simultaneous transcranial views, coronal, horizontal, 3-D rendering and saggital, from a 14-cm deep 3-D scan. (a) Coronal view through the midcerebral fissure (MCF) and atria of the lateral ventricles (ALV) compared with (b) coronal anatomical slice (Roberts and Hanaway 1970, reprinted with permission,). (c) Horizontal image plane from the 3-D scan including the contralateral skull bone, echoes from the body (BLV) and atria of the lateral ventricles (ALV), compared with (d) anatomical section. (e) Real-time 3-D rendered image of the body of the lateral ventricles (BLV) compared with (f) anatomical section. (g) C-scan image of a saggital plane compared with (h) anatomical section. Blunt arrows = orientation of B-scans; arrowheads = volume of rendered image; arrows = depth of C-scan.

Sheep study

With the transducer array on the left side of the sheep skull pointing in an inferior direction toward the circle of Willis, a bolus of US contrast agent (Levovist®) was injected into the right ICA during 3-D color flow Doppler imaging. Figure 8 shows four simultaneous transcranial views from a 10-cm deep 3-D scan, coronal, horizontal and two saggital image planes at depths of 9 and 10 cm. The yellow lines show the 3-D color Doppler regions. The coronal view (Fig. 8a) and horizontal view (Fig. 8b) show brain parenchyma and indicate flow on the right side of the brain in opposite directions through

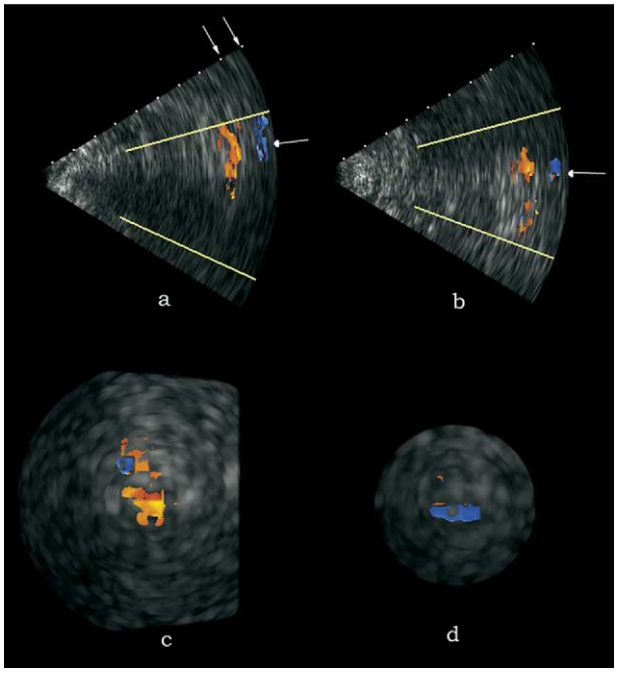

Fig. 8. Four simultaneous transcranial views from a 10-cm deep 3-D scan with color Doppler, including: (a) Coronal, (b) horizontal and two saggital image planes at depths of (c) 9 cm and (d) 10 cm. Arrows = depth of C-scans; blunt arrows = orientation of B-scans.

two discrete vessels at 9 and 10 cm from the transducer. The flow in the coronal image (Fig. 8a) shows the appearance of a long axis segment of the blood vessels, and the orthogonal horizontal scan (Fig. 8b) has the appearance of a short axis of the vessels. The C-scan (saggital) planes positioned over these targets confirm the flow, albeit with degraded spatial resolution.

Figure 9 shows analogous transcranial images after bolus injection of 100 mL of agitated saline into the right ICA, including three simultaneous views from a 10-cm deep 3-D scan, coronal (Fig. 9a), horizontal (Fig. 9b) and saggital (Fig. 9c). The images indicate widespread perfusion superimposed over the echo data from the tissue parenchyma.

DISCUSSION

We have tested the feasibility of real-time 3-D imaging of the brain. In a human subject, the real-time 3-D scans produced simultaneous transcranial axial, coronal and saggital image planes, as well as volume-rendered images of the brain. The images include the gross anatomical landmarks of the brain. The coronal and horizontal B-scan images appear to be comparable with conventional 2-D transskull images, but the C-mode saggital views show reduced spatial resolution due to effects of the skull bone on the transducer beam width. The depth integration of the 3-D rendered image may contain additional information compared with the B-scans.

All of the real-time images exhibit pulsations arising from cerebral blood vessels. Using a bolus injection of contrast agents in a transcranial sheep model, we obtained real-time 3-D color flow Doppler scans and perfusion images through the intact skull.

Our results confirm the feasibility of real-time 3-D transcranial sonography, although these preliminary images may not be of sufficient quality to be clinically useful. The real-time 3-D study should be repeated in a larger trial, with the goals of demonstrating more subtle anatomical features of the brain parenchyma as well as the detection and measurement of cerebrovascular blood flow using venous injection of contrast agent.

A longer-term challenge will be to improve the image quality of transcranial sonograms for both conventional B-scans as well as real-time 3-D. High speed adaptive signal processing will be necessary to correct the phase aberration effects of the skull bone, which degrades the spatial resolution of all transcranial US. Encouraging progress in the correction of US skull aberrations has recently been reported using x-ray computerized tomography (CT) data for large transducer arrays used in focused US therapy (Clement and Hynynen 2002; Aubry et al. 2003).

For such adaptive signal processing, we previously measured the root-mean-square (r.m.s.) phase variations in one dimension across samples of human skull bone from the temporal region using a linear phased array (Smith et al. 1976). The data (averaged over the 13-mm elevation dimension of the array) showed r.m.s. phase variations of 88 ns over a transducer aperture of 6 mm. With our matrix phased array, we can now repeat such measurements in two dimensions, a more important experiment because the skull aberration affects the whole area of every transducer aperture. Our preliminary data from polymer castings of the human temporal bone re-

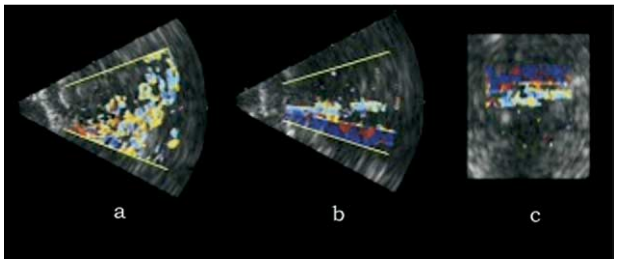

Fig. 9. Three simultaneous transcranial images after the injection of 100 mL of agitated saline into the right internal carotid artery including three simultaneous views from a 10-cm deep 3-D scan: (a) Coronal, (b) horizontal and (c) saggital.

gion have yielded r.m.s. phase variations of 75 ns with a correlation length of only 1.4 mm. Such severe aberration data from the skull bone indicate a huge potential improvement in image quality yet to be realized in real-time transcranial sonography if we can overcome the skull.

Acknowledgements—This research was supported in part by NIH grants (HL 64962 and HL72840). The authors acknowledge the assistance of E. Dixon-Tulloch in the animal experiment.

REFERENCES

Ahmad M, Xie TR, McCulloch M, Abreo G, Runge M. Real-time three-dimensional dobutamine stress echocardiography in assessment of ischemia: Comparison with two-dimensional dobutamine stress echocardiography. J Am Coll Cardiol 2001;37:1303–1309.

Aubry JF, Tanter M, Pernot M, Thomas JL, Fink M. Experimental demonstration of noninvasive transskull adaptive focusing based on prior computed tomography scans. J Acoust Soc Am 2003;113:84–93.

Bauer A, Bogdahn U, Soldner R, Hutzelmeyer A, Haase A. Three-dimensional transcranial duplex sonography with and without contrast enhancement. In: Bogdahn U, Becker G, Schlachetzki F, eds. Echoenhancers and transcranial color duplex sonography. Berlin: Blackwell Science, 1998:141–151.

Becker G, Griewing B. Examination techniques. In: Bogdahn U, Becker G, Schlachetzki F, eds. Echoenhancers and transcranial color duplex sonography. Berlin: Blackwell Science, 1998:219–231.

Berg D, Becker G. Perspectives of B-mode transcranial ultrasound. NeuroImage 2002;15:463–473.

Bogdahn U, Becker G, Schlachetzki F, eds. Echoenhancers and transcranial color duplex sonography. Berlin: Blackwell Science, 1998.

Clement GT, Hynynen K. A non-invasive method for focusing ultrasound through the human skull. Phys Med Biol 2002;47:1219–1236.

Eyding J, Krogias C, Wilkening W, et al. Parameters of cerebral perfusion in phase-inversion harmonic imaging (PIHI) ultrasound examinations. Ultrasound Med Biol 2003;29:1379–1385.

Firek B, Higginbotham M, Russel S, et al. Initial experience with volume-rendered, real-time three dimensional echocardiography in right ventricular endomyocardial biopsy (Abstr.). Eur Heart J 2000;21:3064.

Gahn G, von Kummer R. Ultrasound in acute stroke: A review. Diagn Neuroradiol 2001;43:702–711.

Johnson JI, Sudheimer KD, Davis KK, Winn BM. The navigable atlas of the sheep brain. http://www.msu.edu/user/brains/sheepatlas/, NSF grants IBN 0131267, 0131826, 0131028.

Light ED, Davidsen RE, Fiering JO, Hruschka TA, Smith SW. Progress in 2-D arrays for real-time volumetric imaging. Ultrason Imaging 1998;20:1–16.

Qin JX, Jones M, Shiota T, et al. Validation of real-time three-dimensional echocardiography for quantifying left ventricular volumes in the presence of a left ventricular aneurysm: In vitro and in vivo studies. J Am Coll Cardiol 2000;36:900–907.

Roberts M, Hanaway J. Atlas of the human brain in section. Philadelphia: Lea and Febiger, 1970.

Schlachetzki F, Hoelscher T, Ullrich OW, Schalke B, Bogdahn U. Dynamic and three-dimensional transcranial ultrasonography of an arachnoid cyst in the cerebral convexity. J Neurosurg 2001;94:655–659.

Schmidt MA, Ohazama CJ, Agyeman KO, et al. Real-time three-dimensional echocardiography for measurement of left ventricular volumes. Am J Cardiol 1999;84:1434–1439.

Smith SW, Lopez H, Bodine WJ. Frequency independent contrast-detail analysis. Ultrasound Med Biol 1985;11:467–477.

Smith SW, Pavy HE, von Ramm OT. High speed ultrasound volumetric imaging system part I: Transducer design and beam steering. IEEE Trans Ultrason Ferroelec Freq Control 1991;38:100–108.

Smith SW, Phillips DJ, von Ramm OT, Thurstone FL. Some advances in acoustic imaging through skull. In: Linzer M, ed. Ultrasonic tissue characterization II NBS Pub 525, U.S. Department of Commerce, Washington, DC. 1978a:209–218.

Smith SW, Trahey GE, von Ramm OT. Phased array ultrasound imaging through planar tissue layers. Ultrasound Med Biol 1986;12:229–243.

Smith SW, von Ramm OT, Kisslo JA, Thurstone FL. Real-time ultrasound tomography of the adult brain. Stroke 1978b;9:117–122.

Tsujino H, Jones M, Shiota T, et al. Real-time three-dimensional color Doppler echocardiography for characterizing the spatial velocity distribution and quantifying the peak flow rate in the left ventricular outflow tract. Ultrasound Med Biol 2001;27:69–74.

von Ramm OT, Smith SW, Pavy HE. High speed ultrasound volumetric imaging system part II: Parallel processing and display. IEEE Trans Ultrason Ferroelec Freq Control 1991;38:109–115.